Iranian Journal of Veterinary Surgery

ORIGINAL ARTICLE

Enhancing Infectious Wound Healing in Wistar Rats Using Electrospun Fibrous Membrane Incorporating *Eucalyptus camaldulensis* Extract and Polyvinyl Alcohol

Ali Ashrafian[1], Hamid Reza Moslemi ✉[1], Khatereh Kafshdouzan[2], Mohammad Sadegh Nourbakhsh[3], Sahar Ghaffari Khaligh[2]

[1] Department of Clinical Sciences, Faculty of Veterinary Medicine, Semnan University, Semnan, Iran. [2] Department of Pathobiology, Faculty of Veterinary Medicine, Semnan University, Semnan, Iran. [3] Faculty of Materials and Metallurgical Engineering, Semnan University, Semnan, Iran.

ARTICLE INFO

Article History:

Received: 8 December 2023
Revised: 9 January 2024
Accepted: 13 February 2024

Keywords:

Electrospinning
Healing
Infectious wound
Eucalyptus camaldulensis extract

ABSTRACT

This study explores the potential of electrospun polyvinyl alcohol (PVA) incorporating *Eucalyptus camaldurensis* extract (ELE) as an innovative wound dressing strategy to address the escalating threat of antibiotic resistance and associated complications in bacterial infections of wounds. The investigation is grounded in the recognition of the antibacterial properties inherent in medicinal plants and the advantageous release characteristics of nanomaterials, particularly electrospun nanofibers that closely mimic the extracellular matrix. Utilizing the electrospinning technique, nanofiber mats were fabricated with hydroalcoholic Eucalyptus camaldulensis extract, and their structural and morphological attributes were comprehensively characterized using scanning electron microscopy (SEM), Fourier-transform infrared (FTIR) spectroscopy, and X-ray diffraction (XRD). The study employed 60 male Wistar rats, categorizing them into groups treated with PVA/ELE, nitrofurazone, normal saline, and PVA wound dressings. Microbial and histopathological analyses were conducted at specified intervals post-infection. The results unveiled the remarkable antibacterial efficacy of PVA/ELE, as evidenced by a substantial reduction in bacterial count compared to control groups. Furthermore, the PVA/ELE group demonstrated superior wound size reduction, re-epithelization, and collagen deposition, akin to the effects observed in the nitrofurazone group. The findings suggest that PVA/ELE exhibits significant antimicrobial potential and promotes advanced wound-healing processes. Consequently, this electrospun nanofiber formulation, enriched with ELE, emerges as a promising and viable alternative for conventional wound care, offering multifaceted benefits in combating bacterial infections and facilitating wound healing.

Introduction

In recent years, there has been an increasing focus on enhancing wound healing agents. The management of infectious wounds poses a significant global health concern. Infection is recognized as a crucial factor responsible for prolonging the wound healing process.[1] Gram-positive bacteria, particularly *S. aureus*, have been identified as the main culprits responsible for wound infections.[2,3] In recent years, herbal medicine has garnered considerable attention for its potential in this regard. Essential oils (EOs), known for their antimicrobial properties, exhibit activity not only against bacteria but also against fungi, protozoa, and viruses, which is particularly valuable in cases of mixed infections involving wound sites.[4] The wound dressing is described as a sterile compact barrier that keeps the injured

✉ Corresponding author. Email: h.moslemi@semnan.ac.ir

https://doi.org/10.30500/ivsa.2024.428433.1382

epidermal tissues protected from outside and accelerates the healing process.

An ideal wound dressing should serve multiple functions. It needs to shield the wound from harmful microorganisms, maintain a moist environment to prevent dryness, reduce surface necrosis, and allow oxygen to permeate without causing dehydration. Additionally, it should be comfortable to wear and minimize the risk of mechanical trauma. Moreover, when selecting materials for wound dressing fabrication, important factors to consider include low toxicity, biodegradability, and biocompatibility.[1] The antimicrobial properties of wound dressings containing essential oils and plant extracts have been well-documented in previous studies. However, one of the challenges in utilizing EOs in wound dressings is their limited water solubility, hydrophobic nature, and volatility, which hinder their suitability for pharmaceutical applications.[5] The application of nanotechnological approaches has shown promise in enhancing the efficacy of various therapeutics, including herbal products. By harnessing the nanostructure of plant extracts and their phytochemical constituents, their bioavailability can be increased, and controlled release systems can be developed for sustained delivery at the wound site. This can potentially enhance the permeability of these therapeutic agents into the underlying layers of the skin, which is crucial for facilitating the healing process.[6,7]

In recent scientific literature, the wound-healing potential of numerous essential oils and extracts has been investigated in various animal models. However, limited research has been conducted on the wound-healing effects of herbal medicines utilizing nano-sized drug delivery systems. This area remains relatively unexplored in the existing literature, highlighting the need for further investigations to evaluate the therapeutic efficacy of nano-sized drug delivery systems in facilitating wound healing for herbal medicine applications.[8]

Eucalyptus, a member of the Myrtaceae family originally from Australia, is now widely distributed worldwide, including in Iran. The leaves of this plant possess diverse biological activities attributed to their chemical constituents, such as analgesic, anti-inflammatory, antibacterial, antifungal, and antioxidant properties.[9,10] Incorporating Eucalyptus leaf extract (ELE) into a nanofibrous scaffold offers a dual mechanism for preventing bacterial growth both physically and chemically. The nanofibrous structure with its small pores acts as a physical barrier, preventing the entry of microsized bacteria. Simultaneously, the controlled release of ELE from the scaffold inhibits bacterial growth on the surface of the nanofibrous mat, further supporting wound healing.[11]

A wide array of nanotechnological approaches has been devised for the fabrication of nanofibers, among which electrospinning stands out as an especially remarkable technique. The popularity of electrospinning is attributed to its straightforward implementation, cost-effectiveness, versatility, and exceptional ability to precisely control both fiber diameter and alignment. These advantages have garnered significant attention and made electrospinning a prominent choice in the field of nanofiber development.[6,12,13]

Polyvinyl alcohol (PVA) has gained widespread popularity as a preferred material for fiber fabrication in diverse applications, notably wound dressing scaffolds. This preference is attributed to its exceptional thermal stability, biocompatibility, non-toxicity, easy preparation, water solubility, electrospinnability, and drug delivery capabilities.[14,15] Such advantageous properties position PVA as an ideal choice for biomedical applications, particularly in the development of advanced wound dressings.

To the best of our knowledge, there is a paucity of comprehensive research on the characterization of electrospun composite mats incorporating Eucalyptus leaf extract. Consequently, the primary objective of this study was to develop a novel wound dressing utilizing a nanofibrous scaffold composed of PVA/ELE. Furthermore, the antibacterial activity and wound-healing acceleration potential of the PVA/ELE nanofiber mats were evaluated using an infectious wound model involving *Staphylococcus aureus*.

Materials and Methods

Preparation of Extract

Fresh leaves of *Eucalyptus camaldulensis* were carefully collected from Semnan (Iran), and their species were verified and documented at the herbarium of the Semnan Agriculture and Natural Resources Research Center. The collected leaves were thoroughly washed and dried under dark conditions without the application of heat, after which they were powdered using an electric grinder. A total of 30 gr of the prepared powder was placed in a filter paper thimble and inserted into the extraction chamber of a Soxhlet apparatus. Extraction was carried out using 250 ml of ethanol (80% v/v) at a temperature of 70 °C for 4 hours. The resulting solution was then transferred to a rotary evaporator (model STRIKE300; Wings Company; Italy) to remove the solvent and concentrate the extract. To separate the liquid extract from the solid residue, vacuum filtration was performed using sterile cellulose nitrate membrane filters (0.45 µm). Finally, the liquid extracts were stored in sterile glass containers at a temperature of 4 °C to maintain their integrity and purity.[16]

Minimum Inhibitory Concentration (MIC) Measurement

The strain of *S. aureus* used in this study was isolated from a wound infection obtained from the microbiological laboratory of a Medical Center in Tehran. The identification of the strain was conducted following established clinical microbiology guidelines. As a reference strain, *S. aureus* PTCC 1112 was utilized.

To determine the Minimum Inhibitory Concentration (MIC) of *Eucalyptus camaldulensis* leaf extract against *S. aureus*, the broth micro dilution method was employed. The extract was diluted in Mueller Hinton Broth (MHB) up to a concentration of 6 mg/ml. Approximately 5×10^5 CFU/ml of adjusted *S. aureus* was then added to each well. Positive and negative controls were prepared, with one containing inoculated media without the extract and the other containing sterile medium with the extract.[14] The contents of the wells were gently mixed for 2 minutes using a microplate reader equipped with a shaker (BioTek® Instruments Inc., Winooski, VT, USA), and the absorbance was measured at 630 nm immediately after mixing. Subsequently, the plates were aerobically incubated at 35 °C for 18-20 hours, and the absorbance was re-measured at OD630. Bacterial growth and turbidity were indicated by an increase in absorbance of ≥ 0.1 compared to the initial reading at 0 hours. The MIC was defined as the last dilution at which the growth of the organism was inhibited.[4]

In vitro Antioxidant Activity Using DPPH Assay

The extract's ability to donate hydrogen atoms or electrons was assessed by observing the reduction in color of a purple methanol solution containing 2,2-diphenyl-1-picrylhydrazyl (DPPH). This method, based on the technique developed by Burits and Bucar in 2000, involved using the stable radical DPPH as a reagent in a spectrophotometric assay. In brief, 50 µL of the extract was mixed with 5 mL of a DPPH solution (0.004% methanol solution). After allowing the mixture to incubate at room temperature for 30 minutes, the absorbance was measured at 517 nm against pure methanol. The radical-scavenging activity of the sample was quantified as an inhibition percentage using the following formula: $I\% = ((A_{blank} - A_{sample})/A_{blank}) \times 100$, where A_{blank} is the absorbance of the control (containing all reagents except the test compound), and A_{sample} is the absorbance of the test compound. The concentration of the extract needed to achieve 50% inhibition (IC50) was calculated from the plot of inhibition percentages against the extract using PHARM/PCS-version 4.[17]

Fabrication of ELE-Loaded Nanofibers

A homogeneous solution of PolyVinyl Alcohol (PVA) with a molecular weight of 72,000 (Merk, Germany) was prepared by dissolving it in 10% w/v of distilled water and stirring at 80 °C for 3 hours. The ELE solution was then prepared in distilled water at a concentration of 100 mg/ml. Subsequently, a blend of PVA and ELE solutions was prepared in varying proportions: 100:0, 90:10, 80:20, and 70:30 (v/v).

The electrospinning process was carried out under specific conditions, including a voltage of 15 kV, a distance of 18 cm between the needle tip and collector, and a feed rate of 2.5 ml/h at 300 rpm. This allowed for the formation of nanofibrous films. The final concentrations of ELE incorporated into each film were 10, 20, and 30 mg/ml, providing different levels of ELE content in the resulting films.[14]

Characterizations of Electrospun Wound Dressing

Following the electrospinning process, the dressings underwent SEM testing at the Materials and Metallurgy Laboratory of Amirkabir University of Technology. This analysis aimed to assess the morphology and microstructure of the fabricated samples. Imaging was performed utilizing the XL30 scanning electron microscope manufactured by Philips in the Netherlands, operating at a voltage of 15KV.Subsequently, SEM micrographs at 30× original magnification were evaluated using the ImageJ software (Bethesda, MD, USA) to determine the average fiber diameter and porosity across various layers. The calculation of scaffold porosity in different layers followed the method as recently outlined by Alhosseini *et al*.[18]

For FTIR analysis, the sample was dispatched to the Faculty of Chemistry at Semnan University. The analysis involved Fourier transform infrared analysis (FTIR) and was conducted using a Nicolet 17DSX FT-IR spectrometer, spanning the wave number range of 400-4000/cm. The FTIR analysis aimed to identify and characterize specific chemical groups within both PVA and eucalyptus. Furthermore, the samples were sent to the Nano Research Laboratory at Semnan University's Faculty of Materials and Metallurgy for XRD testing. In this particular test, the crystal structure of the samples was examined via wide-angle X-ray diffraction (XRD) employing a Rotorflex RU200B XRD instrument manufactured by Rigaku, Japan. The XRD utilized X-ray diffraction with nickel-filtered copper (k ¼ = 1.5402 Å). After thorough analysis and verification of the electrospun scaffold composition, the production of the necessary size of wound dressing was carried out.

Animals

The study included a total of 60 male Wistar rats, each weighing approximately 300 g and aged around 4 months. To minimize stress and allow for acclimatization, the rats

were not subjected to any experimental procedures for one week upon arrival. Throughout the study, all animals were housed under uniform environmental conditions and provided with a standard laboratory animal diet. An adequate water supply was ensured with free access to water. Ethical considerations were strictly adhered to, following the guidelines outlined by the US National Health guidelines, and the study protocol was approved by the Ethics Committee of Semnan University, Iran (Code: IR.SU.REC.E-97/09).

Micro-Organisms and Preparation of Inoculum

Staphylococcus aureus, a bacterial strain for which the minimum inhibitory concentration had been previously determined, was prepared at a concentration of 10^6 colony-forming units (CFU) as per the instructions provided by Moslemi *et al*.[19] This standardized concentration was utilized for infecting the wounds in the experimental model.

Circular Excision Wound Model

The rats were subjected to intraperitoneal anesthesia using a combination of 10% ketamine hydrochloride (50 mg/kg) and 2% xylazine hydrochloride (5 mg/kg). Subsequently, the dorsal inter-scapular region of each rat was shaved, and the operation sites were aseptically prepared using povidone-iodine and a 70% ethanol solution. A circular incision with a diameter of approximately 15 mm was carefully made on the skin, leaving the wounds open. Following the skin wounding, the rats received a local inoculation of 1×10^6 CFU of *S. aureus* at the sites of the wounds. After 24 hours of bacterial injection, the rats were divided into four groups: (i) control group, where wounds were treated with normal saline, (ii) PVA group, where wounds were treated with PVA dressing, (iii) PVA/ELE group, where wounds were treated with PVA/ELE nanofibrous electrospun dressing, and (iv) Nitro group, where wounds were treated with nitrofurazone 0.2% (Behvazan Co., Iran).

Tissue Preparation and Evaluation of Antimicrobial Properties

The process of tissue preparation and assessment of antimicrobial activity was conducted following the method described by Stratford *et al*.[20] Under completely sterile conditions, we collected punch biopsy samples from the sides of each wound site. Next, we measured the weight of the tissue samples and proceeded to homogenize them in Brain Heart Infusion (BHI). Consequently, we create serial dilutions with a factor of 10 in a sterile test tube. The tubes were incubated at 35 °C for 24 h. Following the incubation period, 100 microliters of each dilution were cultivated on plate count agar. The plates underwent a meticulous inspection to detect colonies falling within the range of 30 to 300, and subsequently, a count was performed. To enhance precision, each sample was replicated three times. To ensure a consistent count, additional plates were created as duplicates. Subsequently, the colony counts obtained were converted into colony-forming units per gram (CFU/gr) using the provided formula:[19]

$$\text{CFU/gr} = \frac{\text{Colony counts} \times 50 \times \text{Dilution factor}}{\text{Specimen weight (gr)}}$$

Wound Size Reduction

The wound size on each animal was measured on days 7, 14, and 21 after the surgeries. To determine the percentage of wound contraction, the measurements of the wound size were taken both at the time of the surgery and at the time of the biopsy. The formula for calculating wound contraction % is:

$$\%\text{wound contraction} = [(A_o - A_t)/A_o] \times 100,$$

where A_o is the original wound area and A_t is the wound area at the time of biopsy.

Histopathologic Assessments

Histopathologic investigations were conducted to examine the effects of the procedure on the wound healing process. At 7, 14, and 21 days following the operation, the animals were euthanized using an overdose of thiopental sodium. Biopsy specimens from the wound site as described above, were collected for each group. These samples were then fixed in 10% buffered formalin, dehydrated, embedded in paraffin, and subjected to staining with hematoxylin and eosin (H&E) as well as Masson's trichrome stain. Subsequently, the stained specimens were microscopically evaluated to analyze the histopathologic alterations occurring during wound healing.

To ensure unbiased assessment, three sections were randomly chosen from each sample and were blindly evaluated to assess extent and severity of inflammation, angiogenesis, fibroplasia, and the density of mature collagen fibers by three independent assessors. The wound healing process was scored based on Gal et al.'s grading system.[21] The average score was calculated and utilized for comparison.

Statistical Analysis

The statistical analysis was conducted using the SPSS software version 16, employing the Kruskal-Wallis test and independent t-test. Descriptive statistics were used to present the data, with the mean ± standard deviation (SD) being reported. Statistical significance was determined when the p-value was less than 0.05 ($p < 0.05$).

Results

Morphology of PVA and PVA/ELE

Figure 1 illustrates the structural characteristics of nanofiber scaffolds fabricated using pure PVA and PVA blended with ELE at varying ratios. Our findings indicate that when ELE is incorporated in the ratios of 90:10 (v/v) and 80:20 (v/v), the resulting nanofibers exhibit a smooth and slender morphology devoid of any irregularities, suggesting effective integration of ELE extracts within the nanofibrous matrix. However, at a ratio of 70:30 (v/v), a reduction in uniformity and surface smoothness is observed. This variation could be attributed to the increased viscosity and solute concentration, which in turn impacts the nanofiber morphology. Based on this observation, the PVA/ ELE blend at a ratio of 80:20 (v/v) was chosen for subsequent analysis.

In this investigation, we examined the average diameter of electrospun nanofiber scaffolds composed of pure polyvinyl alcohol (PVA) and PVA blended with ELE at varying volumetric ratios (90:10, 80:20, and 70:30). The determined average diameters for pure PVA and PVA/ELE nanofiber scaffolds were 205.4 nm, 231.9 nm, 266.2 nm, and 288.4 nm, respectively.

The results of our study reveal a notable trend wherein an increased concentration of ELE within the blended scaffolds corresponds to a concomitant increase in fiber diameter. Specifically, the average diameter of the electrospun nanofibers consistently rises as the volumetric ratio of ELE in the PVA matrix increases. This observed correlation between ELE concentration and fiber diameter has implications for the structural characteristics of the resulting nanofiber scaffolds, providing valuable insights into the modulation of fiber dimensions through the incorporation of bioactive constituents.

These findings contribute to the understanding of the electrospinning process and its outcomes when utilizing ELE as an additive in PVA-based nanofiber scaffolds. The controlled manipulation of fiber diameter through the modulation of ELE concentrations offers potential applications in tailoring the physical properties of electrospun nanofibrous materials for diverse biomedical and functional purposes.

FTIR Analysis

The FTIR analysis of the eucalyptus extract revealed a range of distinctive peaks, each offering insights into the extract's chemical composition: The peak at 3391.15/cm was associated with O-H bonds, typically found in phenols and alcohols, and exhibited both asymmetric and symmetric tension vibration modes. At 1607.38/cm, a peak indicated the presence of N-H (NH2) and C=C (alkene) bonds, involving bending and stretching vibrational modes. Another peak at 1516.50/cm suggested the existence of N=O (NO2) and C=C (aromatic) bonds. A bond at 1405.42/cm was linked to -C-H (CH3) bending. In the range of 1269.73-107.98/cm, various stretching vibrations were observed, associated with C-X, SO, C-N (NH2), and C-O (OH, COOH) bonds. The presence

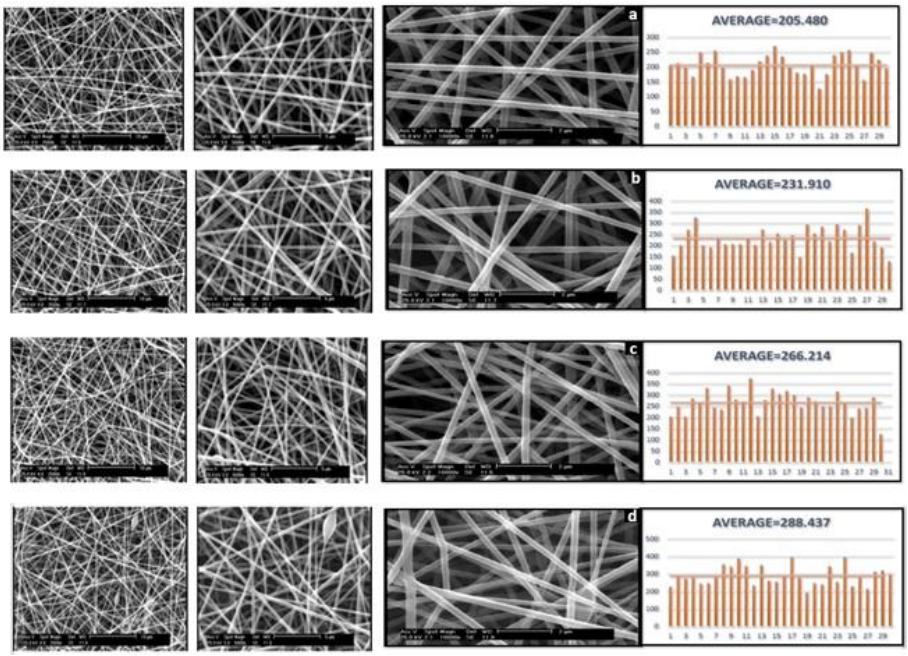

Figure 1. The mean diameters of nanofiber scaffolds fabricated from pure polyvinyl alcohol (PVA) (a), and PVA blended with *Eucalyptus camaldurensis* (ELE) at volumetric ratios of 90:10 (b), 80:20 (c), and 70:30 (d) were determined to be 205.480 nm, 231.910 nm, 266.214 nm, and 288.437 nm, respectively. The final concentration of the ELE incorporated into each film was 10, 20, and 30 mg/ml, respectively.

of -C-H bonds in an aromatic structure was indicated by the peak at 863.29/cm, involving bending. Additionally, peaks at 680.02 and 529.40/cm were attributed to C-X bonds, which are commonly found in halogen-containing compounds. These findings provide a comprehensive overview of the chemical constituents within the eucalyptus extract, shedding light on its potential applications and properties in various contexts (Figure 2a).

The FTIR analysis of polyvinyl alcohol (PVA) revealed distinctive spectral characteristics, offering valuable insights into its chemical composition. Notable findings from the FTIR analysis of PVA include the presence of PVA peaks at 829, 1110, 1731, 2925, and 3185/cm, signifying various vibrational modes and stretching frequencies associated with C-C vibration stretching in the alkyl chain, C-O stretching, C=O stretching, and C-H vibration in alkyl groups. Additionally, at 2950/cm, the symmetric and asymmetric bands related to (CH2-) groups were identified. Moreover, a peak at 1720/cm was linked to C=O stretching, while the 1082/cm peak corresponded to the (O-C) group. The appearance of a distinct peak at 845/cm was associated with C-C vibration. These FTIR results provide a comprehensive understanding of the chemical makeup of PVA, contributing valuable information for various research and industrial applications (Figure 2b).

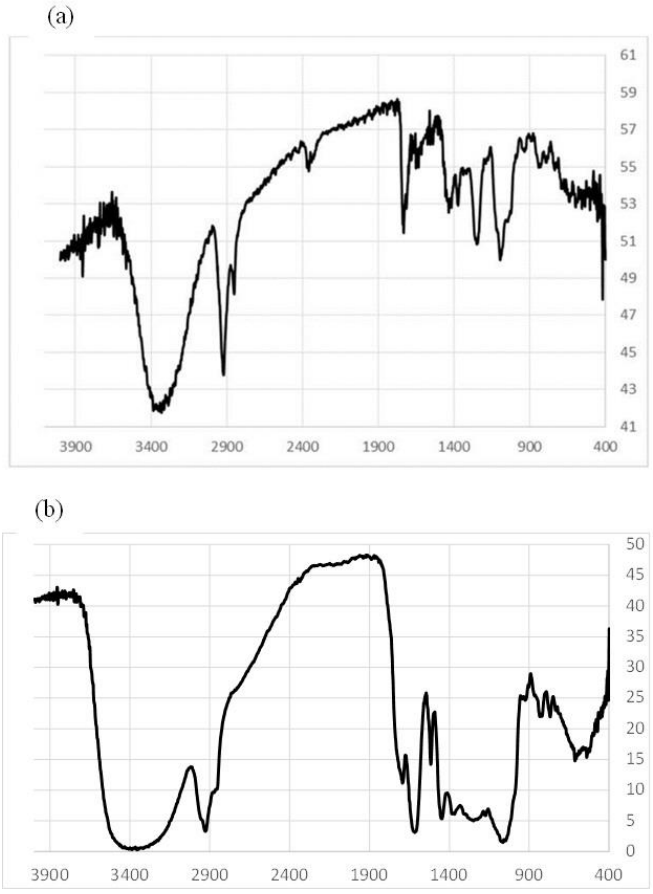

Figure 2. Fourier transforms infrared spectra of (a) PVA/ELE, and (b) PVA nanofbers (0.8:20 mg/ml).

XRD Analysis

The X-ray diffraction (XRD) analysis of eucalyptus fibers was conducted to examine the crystallinity of eucalyptus. The XRD spectrum, as presented in the figure, reveals distinct patterns, providing valuable insights into the structural characteristics of eucalyptus oil. Notably, the XRD spectrum exhibits a prominent, sharp peak at approximately 2θ = 22.6°, accompanied by a secondary, albeit weaker diffraction peak at around 2θ = 15.6°, which can be ascribed to the (002) plane of eucalyptus oil. Furthermore, the primary diffraction peaks are observed at 2θ = 17.5° and 28°, corresponding to the (110) and (200) diffraction planes, respectively. An intriguing observation arising from the XRD analysis is that chemical and mechanical methods applied during the study did not appear to influence the crystal structure of eucalyptus oil. These findings offer a comprehensive understanding of the crystalline nature of eucalyptus fibers and their resilience to external processing methods, contributing to the broader body of knowledge in this field (Figure 3).

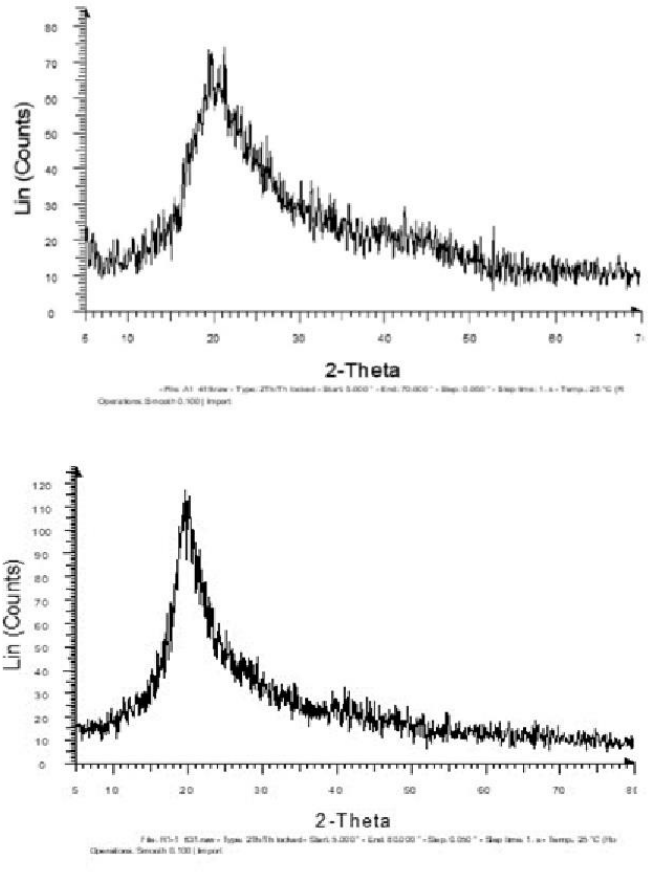

Figure 3. XRD pattern of (a) PVA/ELE nanofbers, (b) PVA (0.8:20 mg/ml).

Characterization of the Extract

The hydro-alcoholic extract of *E. camaldulensis* leaves exhibited a minimum inhibitory concentration of 3mg/ml against *S. aureus* when assessed using the microdilution method. The *in vitro* antioxidant activities of *E.*

camaldulensis leaves extract and beta-hydroxy toluene (BHT) in the DPPH assay were found to be 0.0008 µg/ml and 4.9 µg/ml, respectively. Notably, the extract exhibited higher free radical-scavenging activities compared to BHT. High IC50 values indicated low antioxidant activity.

Antibacterial Examination

To determine the bacterial load in different study groups, the number of bacteria isolated from wounds was quantified following the protocol outlined by Stratford et al. The results, presented in Table 1, revealed that the Nitro group had a significantly lower bacterial count compared to the other groups ($p \leq 0.05$). Conversely, both the control and PVA groups displayed significantly higher bacterial counts compared to the other groups ($p \leq 0.05$). Moreover, the number of bacteria in the Nitro group was significantly lower than that in the PVA/ELE group ($p \leq 0.05$). These findings demonstrate that the combination of the extract with nanofibers effectively reduced bacterial growth compared to the control group.

During the second week of analysis, the bacterial count in all groups exhibited a decrease compared to the count on the seventh day. Specifically, on the 14th day, the Nitro group had a significantly lower number of bacteria compared to the other groups ($p \leq 0.05$). Notably, the PVA/ELE group showed a significant reduction in bacterial growth compared to both the control and PVA groups ($p \leq 0.05$).

The decline in bacterial counts persisted across different groups until the 21st day. Notably, both the Nitro and PVA/ELE groups exhibited significantly lower bacterial counts compared to the control and PVA groups ($p \leq 0.05$). However, there was no notable difference in bacterial counts between the control and PVA groups, suggesting that PVA nanofibers likely lack antimicrobial effects ($p \leq 0.05$).

Wound Size Reduction

Throughout the progression of wound healing, alterations in wound size were quantified to determine the rate of wound size reduction, as demonstrated in Table 2. Notably, wounds subjected to normal saline and PVA nanofiber treatment exhibited a comparatively slower closure rate in contrast to other experimental groups. By the seventh day, all wounds demonstrated initiation of healing with partial closure ranging from 21 ± 0.71 to 40 ± 0.47%. Subsequently, by day 14, subjects treated with nitrofurazone and PVA/ELE displayed a superior reduction in wound size compared to control groups. Ultimately, on day 21, all wounds exhibited closure rates ranging from 93 ± 0.75 to 98 ± 0.83%. Notably, among the experimental groups, nitrofurazone, and PVA/ELE were identified as more efficacious in promoting wound size reduction (Figure 4).

Table 1. Mean ± SD of the bacterial counts (CFU/gr) in all groups following infection with *S. areous* on days 7, 14, and 21.

Days post infected	7	14	21
PVA/ELE (0.8:20 mg/ml)	$4.08 \pm 0.6 \times 10^{6\,a}$	$6.7 \pm 2.25 \times 10^{5\,a}$	$2.92 \pm 0.75 \times 10^{5\,a}$
Nitrofurazone	$2.8 \pm 0.7 \times 10^{6\,b}$	$3.8 \pm 0.49 \times 10^{5\,b}$	$1.46 \pm 0.27 \times 10^{5\,b}$
PVA	$2.97 \pm 1.2 \times 10^{7\,c}$	$3.7 \pm 1.6 \times 10^{6\,c}$	$2.82 \pm 0.1 \times 10^{6\,c}$
Control	$8.37 \pm 11.7 \times 10^{7\,c}$	$5.3 \pm 1.2 \times 10^{6\,d}$	$2.66 \pm 0.11 \times 10^{6\,c}$

There are significant differences in values with non-identical superscripts in each column ($p < 0.05$).

Table 2. Mean ± SD of the wound size reduction in all groups

Days post infected	7	14	21
PVA/ELE	40.72 ± 0.47	95.31 ± 0.71	98.34 ± 0.83
Nitrofurazone	21.31 ± 0.71	87.53 ± 0.67	98 ± 0.81
PVA	22.35 ± 0.83	69.06 ± 1	93.36 ± 0.75
Control	27.61 ± 0.47	80.73 ± 0.47	94.16 ± 0.99

Histopathologic Examination

The histopathologic assessment was employed to evaluate the progress of wound healing in the various groups. The analysis focused on factors such as fibroplasia, angiogenesis, inflammatory cell count, and the density of mature collagen fibers, which collectively determine the extent of healing across the different samples (Table 3). On the 7th day, based on the obtained results, none of the studied groups exhibited epithelialization, leading to the absence of any statistically significant differences in this particular factor. However, moderate to high density of fibroblasts was observed within the granulation tissue, with no statistically significant differences identified between the study groups. Collagen synthesis was observed to occur to a limited extent across all study groups. Notably, a significant difference was found between the PVA/ELE and nitrofurazone groups compared to the PVA nanofibers and control groups in terms of collagen formation. Regarding angiogenesis, a moderate to good rate of blood vessel formation was observed in all study groups. However, the differences between the groups were not statistically significant. The mean count of inflammatory cells did not exhibit a statistically significant difference among the study groups (Figure 5).

After two weeks, significant progress in epithelialization was observed in the PVA/ELE and nitrofurazone groups, while no epithelialization was noted in the PVA nanofiber and control groups. Notably, there was a statistically significant difference in this aspect between the PVA/ELE and nitrofurazone groups compared to the PVA nanofiber and control groups. However, no significant difference was observed between the PVA/ELE and nitrofurazone treatment groups. In

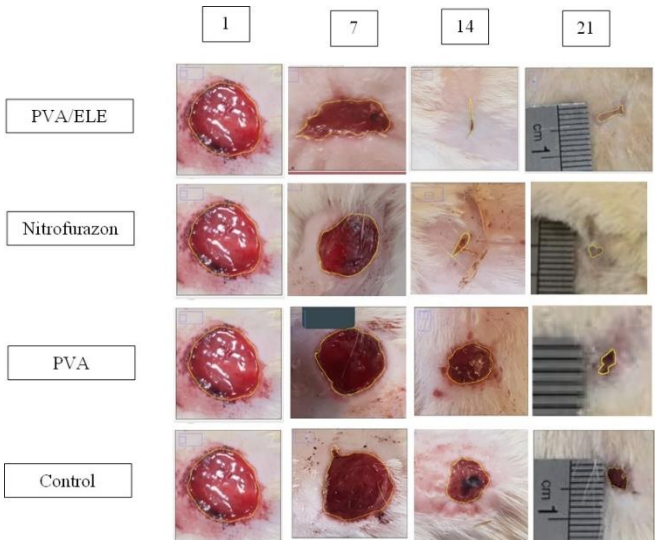

Figure 4 Wound size reduction over 21 days treated with PVA/ELE (0.8:20 mg/ml).

terms of fibroblast density within the granulation tissue, a moderate level was observed in nearly all groups, with no statistically significant differences detected among them. During this period, an increase in both fiber density and collagen thickness was observed. A statistically significant difference was noted between the PVA/ELE and nitrofurazone groups compared to the PVA and control groups in terms of fiber density and collagen thickness. As the wound healing process progressed across all groups, a decrease in angiogenesis within the granulation tissue was observed, although the difference between the groups was not statistically significant. In terms of the inflammatory response, there was no statistically significant difference in the count of inflammatory cells. However, the mean inflammation rate in the PVA/ELE and nitrofurazone groups was lower compared to both the PVA and control groups (Figure 6).

On day 21, notable progress in epithelialization was observed in the nitrofurazone and PVA/ELE treatment groups. However, the epithelialization process in the PVA and control groups was slow and limited to the initial stages. Significantly, there was a notable difference between the PVA/ELE and nitrofurazone treatment groups compared to the PVA and control groups. No significant difference was found between the PVA/ELE and nitrofurazone treatment groups. The density of fibroblasts within the granulation tissue was generally low to moderate in almost all groups, with no statistically significant difference detected. Although the deposition of collagen fibers was denser and thicker in the PVA/ELE and nitrofurazone treatment groups compared to the PVA and control groups, no significant difference was observed between the study groups. As the healing process advanced in all groups, angiogenesis within the granulation tissue decreased. However, there was no significant difference observed between the groups. Regarding the number of inflammatory cells, no statistically significant difference was found. Nevertheless, the mean inflammation rate in the PVA/ELE and nitrofurazone groups was lower than in the PVA nanofiber and control groups (Figure 7).

Table 3. Mean ± SD of the histopathologic parameters in all groups

Histo-pathologic parameters	Inflammatory cell count			Collagen			Angiogenesis			Fibroblasts			Epithelization		
Days post infected	7	14	21	7	14	21	7	14	21	7	14	21	7	14	21
PVA/ELE	2.75 ± 0.5	2.5 ± 1	1.8 ± 0.83	2	2.5 ± 0.57[a]	3.26 ± 0.57	2.5 ± 0.57	1.5 ± 0.7	1.8 ± 1.3	2.75 ± 0.5	3	1.8 ± 1.3	0	3 ± 1.41[a]	4[a]
Nitrofurazone	3.5 ± 0.57	2.75 ± 0.5	2 ± 1	1.75 ± 0.5	2.5 ± 0.57[a]	3 ± 0.7	3.25 ± 0.5	2.5 ± 0.57	2 ± 0.7	3.75 ± 0.5	3	2.2 ± 0.44	0	3.25 ± 0.95[a]	4[a]
PVA	3.25 ± 0.5	3.25 ± 0.5	2.8 ± 0.83	0.5 ± 0.57	1.44 ± 0.41[b]	2 ± 1	3	3 ± 0.81	3 ± 1	3.75 ± 0.5	3.5 ± 0.57	3 ± 1	0	0	0.4 ± 0.45[b]
Control	4	3.43 ± 0.53	3 ± 0.66	1.12 ± 0.83	1.33 ± 0.57[b]	2.2 ± 0.83	2.5 ± .57	2.66 ± 1.15	2.4 ± 0.89	2.75 ± 0.5	3 ± 1.7	2.85 ± 0.83	0	0	0.4 ± 0.89[b]

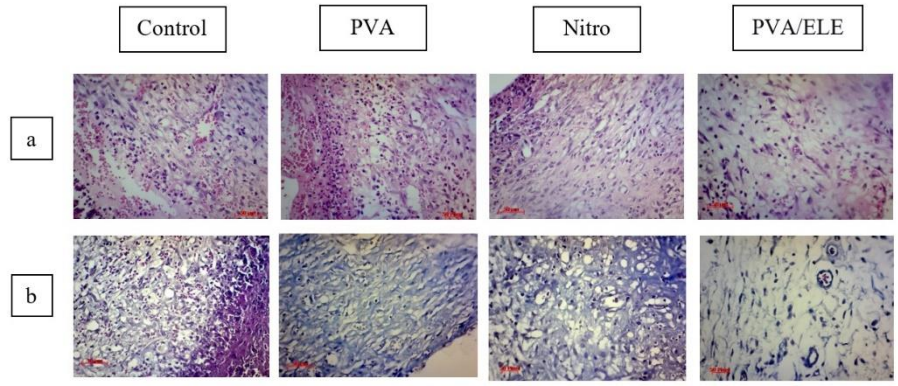

Figure 5. Histopathology of the wound on day 7 by (a) H&E staining (400×). The abundance of newly formed blood vessels, intercellular edema, the presence of inflammatory cells (neutrophils, lymphocytes, and macrophages), fibroblasts, and thin collagen fibers are observed in the image without any special arrangement or orientation, (b) Masson's trichrome staining for collagen estimation (400×). Thin twisted collagen fibers with very low density and completely crossed are seen in all groups.

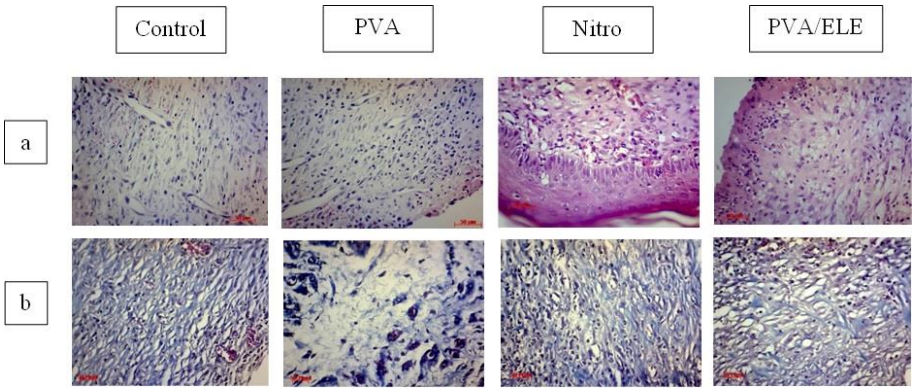

Figure 6. Histopathology of the wound on day 14 by (a) H&E staining (400×). The formation of a well-defined epidermal layer, a relative reduction of newly formed vessels, an increase in the population of fibrocytes to fibroblasts, a decrease in intercellular edema, a decrease in the number of mononuclear inflammatory cells, and relative thickening and relative orientation of collagen fibers can be seen in different groups, (b) Masson's trichrome staining for collagen estimation (400×). The collagen fibers in the PVA/ELE group are seen to be somewhat thickened and aligned, while the collagen fibers are still thin and twisted, without specific orientation and relatively crossed in other groups.

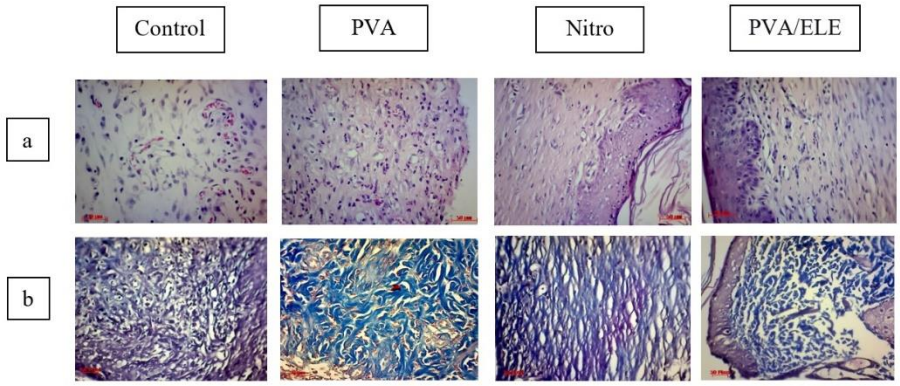

Figure 7. Histopathology of the wound on day 21 by (a) H&E staining (400×). Epithelization and epidermal layer formation in Nitro and PVA/ELE groups is quite clear. The increase in the population of fibrocytes to fibroblasts, the significant reduction of newly formed blood vessels and intercellular edema, the order and orientation and parallel arrangement between thick collagen fibers are clearly evident in all groups, except for the control group. Moreover, the number of mononuclear inflammatory cells can be seen slightly, (b) Masson's trichrome staining for collagen estimation (400×). In the PVA/ELE group, thick, parallel, aligned and high-density collagen fibers can be seen in the image, while although the collagen fibers are thick in the Nitro group, the length of the fibers is short and the misalignment of the fibers is noticeable. Crossed and relatively thin low-density collagen fibers are seen in the PVA and control groups as well.

Discussion

With the rising challenge of antibiotic resistance, bacterial infections in wounds pose serious risks, leading to significant medical and economic burdens. Researchers have addressed this issue by investigating two potential avenues: the use of medicinal plants possessing antibacterial and antioxidant properties, and the utilization of nanomaterials with controlled release capabilities.[6,22] These approaches aim to effectively manage wound infections and promote the process of wound healing. Electrospun nanofibers, with their structural resemblance to the extracellular matrix, have emerged as a promising choice for wound dressings.[14] This study aimed to assess the antibacterial activity and wound-healing promotion effects of an electrospun polyvinyl alcohol (PVA) membrane incorporated with *Eucalyptus camaldulensis* extract on surgical wounds infected with *S. aureus* in Wistar rats. According to Mumtaz *et al*.[9] eucalyptus leaf extracts were found to contain several compounds, including oenothein B, pentagalloyl glucose, tellimagrandin I, gemin D, and pedunculagin. Furthermore, numerous studies have documented the presence of diverse polyphenolic compounds in eucalyptus leaves, including acylphenols and their derivatives, flavonoids, tannins, triterpenoids, and their glycosides. These compounds have been found to possess diverse biological activities, including anti-bacterial, anti-inflammatory, and anti-tumor effects.[9,23] Exploiting these properties, ELE was incorporated into PVA nanofiber scaffolds to impart desirable properties for wound management. Electrospinning was conducted using pure PVA and PVA/ELE solutions in various ratios. Optimal uniform nanofibers of PVA and the appropriate amount of ELE were successfully obtained by maintaining the desired viscosity and concentration during the electrospinning process. Hence, PVA, in combination with the extract, enabled the production of smooth and uniform nanofibers without bead formation at desirable concentrations.[15] In a related study by Aruan et al., they reported the formation of smooth nanofibers in PVA scaffolds loaded with soursop leaf extract, albeit at

different concentrations. The presence of beads was observed when the solution had higher viscosity.[24] Similar observations have been reported regarding the electrospinning of PVA nanofibers in the presence of extracts, where the concentration of the extract significantly influenced fiber formation. For example, scaffolds containing Coptis Chinensis extract exhibited bead formation at higher concentrations.[25] The results of this study showed, higher concentrations of ELE led to an increase in average fiber diameter due to the higher concentration and viscosity of the solution. Consistent with previous studies, higher concentrations of extracts in PVA scaffolds resulted in larger fiber diameters.[24,25] Furthermore, the incorporation of ELE in PVA scaffolds did not significantly alter the prominent intensive peak, attributed to the partially crystalline structure of the extract, while the polyvinyl alcohol scaffold exhibited a single strong intensive peak due to its semi-crystalline structure and intermolecular hydrogen bonds.

Through a comprehensive review of existing literature, it becomes evident that bacterial infections have a detrimental impact on the wound healing process. Such infections can significantly disrupt the healing trajectory by releasing toxins and proteases, consequently prolonging the inflammation phase at the wound site.[3] In This study the analysis of bacterial counts at the wound site on days 7, 14, and 21 after *S. aureus* infection showed a remarkable reduction in bacterial numbers in the PVA/ELE treatment group when compared to both the normal saline and PVA nanofiber groups. This notable disparity in bacterial counts among the experimental groups strongly suggests the antimicrobial efficacy of eucalyptus extract and its compounds. In a study by Alizadeh Behbahani *et al*. the specific antimicrobial effects of eucalyptus leaves against *S. aureus* were investigated, revealing a MIC value of 8 mg/ml for the aqueous extract of eucalyptus leaves against *S. aureus*.[26] In contrast, in our current study, we found a lower MIC value of 3 mg/ml for the eucalyptus extract. This discrepancy can be attributed to differences in the bacterial strain utilized in this study and the specific phytochemical properties of the extract used, as it is known that the habitat of a plant plays a significant role in determining its constituent compounds.[16] Likewise, the antimicrobial efficacy of Eucalyptus against *S. aureus* has been documented in a multitude of scholarly investigations.[27-29] Antimicrobial compounds exhibit their effects by targeting various cellular structures or disrupting multiple chemical bonds. These compounds can induce cell wall destruction, damage the cellular membrane, disrupt proton generator function, inhibit extracellular protease activity, and cause coagulation of cytoplasmic contents.[30]

Furthermore, the histopathological evaluation conducted in this study provided compelling evidence of the beneficial effects of the electrospun nanofibrous mat fabricated from the combination of polyvinyl alcohol and eucalyptus extract. In brief, the histological findings demonstrated that the PVA/ELE scaffold and nitrofurazone groups facilitated faster healing of full-thickness wounds compared to the other groups within the same timeframe. The infected wounds treated with PVA/ELE and nitrofurazone exhibited enhanced and well-structured granulation tissue, improved epithelialization, increased deposition of collagen fibers, and reduced infiltration of lymphocytes and neutrophils. This accelerated healing can be attributed to the antimicrobial and antioxidant activity associated with the ELE extract. Previous studies have extensively demonstrated the remarkable abilities of flavonoids and their derivatives. These compounds are well-known for their capacity to reduce lipid peroxidation, which in turn leads to enhanced vascularity and effectively prevents or slows down cell necrosis. Furthermore, their valuable contribution to wound healing is widely acknowledged, primarily due to their remarkable antimicrobial and astringent properties. These properties play a crucial role in wound contraction and accelerate the epithelization process, facilitating faster and more efficient healing.[31] Additionally, research has highlighted the significance of protection of wounds from inflammation as a crucial factor in accelerating the wound healing process. When tissue injury occurs, the release of reactive oxygen species (ROS) is the initial response, aiming to trigger cell survival signaling and combat invading microorganisms. However, excessive concentrations of ROS can lead to oxidative damage and exacerbate the inflammatory condition of the skin.[32,33] In line with this idea, evidence from both experimental and clinical studies suggests that the inclusion of antioxidants can be a viable approach to neutralizing ROS and promoting the wound healing process.[34]

In this study, the electrospinning technique was successfully utilized to fabricate a continuous nanofibrous structure composed of PVA/ELE. The incorporation of *Eucalyptus camaldulensis* extract (ELE) into the nanofibrous scaffold offered antimicrobial and antioxidant properties, which proved beneficial in managing infected wounds. The results demonstrated that the PVA/ELE nanofibrous blend scaffold effectively inhibited the growth of *S. aureus* and significantly accelerated the wound healing process in the rat model. Given the escalating global concerns surrounding the rise of antibiotic-resistant microorganisms, the use of PVA nanofibrous dressings incorporating medicinal plants with antimicrobial and antioxidant properties holds great promise as a natural and topical therapeutic alternative for clinical wound management. Therefore, it is

recommended to explore the potential of these PVA-based nanofibrous dressings containing plant extracts for broader clinical applications. Further research and clinical trials are warranted to validate their efficacy and safety in a wider range of wound types and patient populations.

Acknowledgments

The authors would like to appreciate Mrs. Reisian at the department of pathobiology, the veterinary medicine of Semnan University for her technical assistance during the procedure of the experiments.

Conflict of Interest

The authors declare no conflict of interest.

References

1. Fahimirad S, Abtahi H, Satei P, Ghaznavi-Rad E, Moslehi M, Ganji A. Wound healing performance of PCL/chitosan based electrospun nanofiber electrosprayed with curcumin loaded chitosan nanoparticles. *Carbohydrate Polymers*. 2021; 1(259): 1-13. doi: 10.1016/j.carbpol.2021.117640
2. Golmohammadi R, Najar-Peerayeh S, Tohidi Moghadam T, Hosseini SM. Synergistic antibacterial activity and wound healing properties of selenium-chitosan-mupirocin nanohybrid system: an *in vivo* study on rat diabetic *Staphylococcus aureus* wound infection model. *Scientific Reports*. 2020; 10: 1-10. doi: 10.1038/s41598-020-59510-5
3. Lindsay S, Oates A, Bourdillon K. The detrimental impact of extracellular bacterial proteases on wound healing. *International Wound Journal*. 2017; 14(6): 1237-1247. doi: 10.1111/iwj.12790
4. Malekpour B, Kafshdouzan K, Javan AJ, Salimi-Bejestani MR. Inhibition of TEM_{bla} producing *Escherichia coli* isolated from poultry colibacillosis using *Cinnamomum camphora* and *Syzygium aromaticum* essential oils. *Avicenna Journal of Clinical Microbiology and Infection*. 2019; 6(3): 88-94. doi: 10.34172/ajcmi.2019.16
5. Mishra P, Gupta P, Srivastava AK, Poluri KM, Prasad R. Eucalyptol/β-cyclodextrin inclusion complex loaded gellan/PVA nanofibers as antifungal drug delivery system. *International Journal of Pharmaceutics*. 2021; 609: 121163-121175. doi: 10.1016/j.ijpharm.2021.121163
6. Hajialyani M, Tewari D, Sobarzo-Sánchez E, Nabavi, SM, Farzaei MH, Abdollahi M. Natural product-based nanomedicines for wound healing purposes: therapeutic targets and drug delivery systems. *International Journal of Nanomedicine*. 2018; 3(13): 5023-5043. doi: 10.2147/IJN.S174072
7. Sriyanti I, Edikresnha D, Rahma A, Munir MM, Rachmawati H, Khairurrijal K. Mangosteen pericarp extract embedded in electrospun PVP nanofiber mats: physicochemical properties and release mechanism of α-mangostin. *International Journal of Nanomedicine*. 2018; 13: 4927-4941. doi: 10.2147/IJN.S167670
8. Alam P, Shakeel F, Anwer MK, Foudah AI, Alqarni MH. Wound healing study of eucalyptus essential oil containing nanoemulsion in rat model. *Journal of Oleo Science*. 2018; 67(8): 957-968. doi: 10.5650/jos.ess18005
9. Mumtaz, R. Zubair, M. Khan, M.A. Muzammil, S. Siddique, M.H. Extracts of *Eucalyptus alba* promote diabetic wound healing by inhibiting *α*-glucosidase and stimulating cell proliferation. *Evidence-Based Complementary and Alternative Medicine*. 2022; 2022: 1-12. doi: 10.1155/2022/4953105
10. Göger G, Karaca N, Buyukkilic B, Demirci B, Demirci F. *In vitro* antimicrobial, antioxidant and anti-inflammatory evaluation of eucalyptus globulus essential oil. *Natural Volatiles and Essential Oils*. 2020; 7(3): 1-11. doi: 10.37929/nveo.759607
11. Edikresnha D, Suciati T, Munir MM, Khairurrijal K. Polyvinylpyrrolidone/cellulose acetate electrospun composite nanofibres loaded by glycerine and garlic extract with *in vitro* antibacterial activity and release behaviour test. *RSC Advances*. 2019; 9(45): 26351-26363. doi: 10.1039/C9RA04072B
12. Xue J, Wu T, Dai Y, Xia Y. Electrospinning and Electrospun Nanofibers: Methods, Materials, and Applications. Chemical Reviews. 2019; 119(8): 5298-5415. doi: 10.1021/acs.chemrev.8b00593
13. Niemczyk-Soczynska B, Gradys A, Sajkiewicz P. Hydrophilic Surface Functionalization of Electrospun Nanofibrous Scaffolds in Tissue Engineering. *Polymers*. 2020; 12(11): 2636-2656. doi: 10.3390/polym12112636
14. Reisi F, Kafshdouzan K, Moslemi HR, Nourbakhsh MS, Ghaffari Khaligh S. the electrospun fibrous membrane containing pomegranate seed extract/polyvinyl alcohol improves infectious wound healing in Wistar rats. *Fibers and Polymers*. 2023; 24(4): 1225-1235. doi: 10.1007/s12221-023-00076-0
15. Fathi A, Khanmohammadi M, Goodarzi A, Foroutani L, Taherian Mobarakeh Z, Saremi J, Arabpour Z, Ai J. Fabrication of chitosan-polyvinyl alcohol and silk electrospun fiber seeded with differentiated keratinocyte for skin tissue regeneration in animal wound model. *Journal of Biological Engineering*. 2020; 14: 1-14. doi: 10.1186/s13036-020-00249-y
16. Hajifattahi F, Moravej-Salehi E, Taheri M, Mahboubi A, Kamalinejad M. Antibacterial effect of hydroalcoholic extract of Punica granatum Linn. Petal on common oral microorganisms. *International Journal of Biomaterials*. 2016; 14: 1-6. doi: 10.1155/2016/8098943
17. Burits M, Bucar F. Antioxidant activity of *Nigella sativa* essential oil. *Phytotherapy Research*. 2000; 14: 323-328. doi: 10.1002/1099-1573(200008)14:5<323::aid-ptr621>3.0.co;2-q
18. Alhosseini SN, Moztarzadeh F, Mozafari M, Asgari S, Dodel M, Samadikuchaksaraei A, Kargozar S, Jalali N. Synthesis and characterization of electrospun polyvinyl alcohol nanofibrous scaffolds modified by blending with chitosan for neural tissue engineering. *International Journal of Nanomedicine*. 2012; 7: 25-34. doi: 10.2147/IJN.S25376
19. Moslemi HR, Hoseinzadeh H, Badouei MA, Kafshdouzan K, Mazaheri-Nezhad-Fard R. Antimicrobial activity of *Artemisia absinthium* against surgical wounds infected by *Staphylococcus aureus* in a rat model. *Indian Journal of Microbiology*. 2012; 52: 601-604. doi: 10.1007/s12088-012-0283-x
20. Stratford AF, Zoutman DE, Davidson JSD. Effect of lidocaine and epinephrine on *Staphylococcus aureus* in a guinea pig model of surgical wound infection. *Plastic and Reconstructive Surgery*. 2002; 110: 1275-1279. doi: 10.1097/01.PRS.0000025427.86301.8A
21. Gal P, Kilik R, Mokry M, Vidinsky B, Vasilenko T, Mozes S, Bobrov N, Tomori Z, Bober J, Lenhardt L. Simple method of open skin wound healing model in corticosteroid-treated and diabetic rats: standardization of semi-quantitative and quantitative histological assessments. *Veterinary Medicine*. 2008; 53: 625-659. doi: 10.17221/1973-VETMED
22. Maliszewska I, Czapka T. Electrospun polymer nanofibers with antimicrobial activity. *Polymers*. 2022; 14(9): 1661-1693. doi: 10.3390/polym14091661
23. Li W, Zhang X, He Z, Chen Y, Li Z, Meng T, Li Y, Cao Y. *In vitro*

and in vivo antioxidant activity of eucalyptus leaf polyphenols extract and its effect on chicken meat quality and cecum microbiota. *Food Research International*. 2020; 136: 1-44. doi: 10.1016/j.foodres.2020.109302
24. Aruan NM, Sriyanti I, Edikresnha D, Suciati T, Munir MM. Polyvinyl alcohol/soursop leaves extract composite nanofibers synthesized using electrospinning technique and their potential as antibacterial wound dressing. *Procedia Engineering*. 2017; 170: 31-35. doi: 10.1016/j.proeng.2017.03.006
25. Yang SB, Kim EH, Kim SH, Kim YH, Oh W, Lee JT, Jang YA, Sabina Y, Ji BC, Yeum JH. Electrospinning fabrication of poly(vinyl alcohol)/coptis chinensis extract nanofibers for antimicrobial exploits. *Nanomaterials*. 2018; 8(9): 734-748. doi: 10.3390/nano8090734
26. Alizadeh Behbahani B, Tabatabaei Yazdi F, Mortazavi A, Zendeboodi F, Gholian MM, Vasiee A. Effect of aqueous and ethanolic extract of *Eucalyptus camaldulensis L*. on food infection and intoxication microorganisms "*in vitro*". *Journal of Paramedical Sciences* 2013; 4(3): 89-99.
27. Bachir RG, Benali M. Antibacterial activity of the essential oils from the leaves of *Eucalyptus globulus* against *Escherichia coli* and *Staphylococcus aureus*. *Asian Pacific Journal of Tropical Biomedicine*. 2012; 2(9): 739-742. doi: 10.1016/S2221-1691(12)60220-2
28. Sugumar S, Ghosh V, Nirmala MJ, Mukherjee A, Chandrasekaran N. Ultrasonic emulsification of eucalyptus oil nanoemulsion: antibacterial activity against *Staphylococcus aureus* and wound healing activity in Wistar rats. *Ultrason. Sonochem*. 2014; 21(3): 1044-1049. doi: 10.1016/j.ultsonch.2013.10.021
29. Elangovan S, Mudgil P. Antibacterial properties of *Eucalyptus globulus* essential oil against MRSA: a systematic review. *Antibiotics*. 2023; 12(3): 474-492. doi: 10.3390/antibiotics12030474
30. Miklasińska-Majdanik M, Kępa M, Wojtyczka RD, Idzik D, Wąsik TJ. Phenolic Compounds Diminish Antibiotic Resistance of *Staphylococcus Aureus* Clinical Strains. *International Journal of Environmental Research and Public Health*. 2018; 15: 2321-2339. doi: 10.3390/ijerph15102321
31. Velmurugan C, Geetha C, Shajahan S, Vijayakumar S, Kumar PL. Wound healing potential of leaves of *Eucalyptus citriodoral* in rats. *World Journal of Pharmaceutical Sciences.* 2014; 2: 62–71.
32. Cano Sanchez M, Lancel S, Boulanger E, Neviere R. Targeting oxidative stress and mitochondrial dysfunction in the treatment of impaired wound healing: a systematic review *Antioxidants*. 2018; 7(8), 98-112. doi: 10.3390/antiox7080098
33. Dunnill C, Patton T, Brennan J, Barrett J, Dryden M, Cooke J, Leaper D, Georgopoulos NT. Reactive oxygen species (ROS) and wound healing: the functional role of ROS and emerging ROS-modulating technologies for augmentation of the healing process. *International Wound Journal*. 2017; 14(1), 89-96. doi: 10.1111/iwj.12557
34. Fitzmaurice SD, Sivamani RK, Isseroff RR. Antioxidant therapies for wound healing: a clinical guide to currently commercially available products. *Skin Pharmacology and Physiology*. 2011; 24(3): 113-126. doi: 10.1159/000322643